Optical Genome Mapping Identifies a Novel Pediatric Embryonal Tumor Subtype with a *ZNF532-NUTM1* Fusion

Miriam Bornhorst, MD[1,2,3,4]*, Augustine Eze, Jr., MS[2,3], Surajit Bhattacharya, PhD[3], Ethan Putnam, BS[2,3], M. Isabel Almira-Suarez, MD[5], Christopher Rossi, MD[5], Madhuri Kambhampati MS[3], Miguel Almalvez, BS[3], Joyce Turner MS[6], John Myseros, MD[7], Eric Vilain, MD, PhD[3,8], Roger J. Packer, MD[2,9], Javad Nazarian, PhD[2,3,8], Brian Rood, MD[1,2,4,10], Hayk Barseghyan PhD[3,8,11]

[1]Division of Hematology/Oncology, Children's National Hospital, Washington, DC 20010, USA
[2]Brain Tumor Institute, Children's National Hospital, Washington, DC 20010, USA
[3]Center for Genetics Medicine Research, Children's National Hospital, Washington, DC 20010, USA
[4]Department of Pediatrics, School of Medicine and Health Sciences, George Washington University, Washington, DC, 20037, USA
[5]Divison of Pathology, Children's National Hospital, Washington, DC, 20010, USA
[6]Division of Genetics and Metabolism, Children's National Hospital, Washington, DC, 20010, USA
[7]Division of Neurosurgery, Children's National Hospital, Washington, DC, 20010, USA
[8]Center for Genomics and Precision Medicine, School of Medicine and Health Sciences, George Washington University, Washington, DC 20037, USA
[9] Center for Neuroscience and Behavioral Medicine, Children's National Hospital, Washington, DC, 20010, USA
[10] Center for Cancer and Immunology Research, Children's National Hospital, Washington, DC, 20010, USA
[11]Bionano Genomics, Inc., San Diego, CA 92121, USA

*Corresponding author

Corresponding Author Contact Information

*Miriam Bornhorst
Email: mbornhorst@childrensnational.org
Children's National Hospital
Washington, DC 20010

Abstract

Molecular characteristics of pediatric brain tumors have not only allowed for tumor subgrouping but have introduced novel treatment options for patients with specific tumor alterations. Therefore, an accurate histologic and molecular diagnosis is critical for optimized management of all pediatric patients with brain tumors, including central nervous system embryonal tumors. We present a case where optical genome mapping identified a *ZNF532-NUTM1* fusion in a patient with a unique tumor best characterized histologically as a central nervous system embryonal tumor with rhabdoid features. Additional analyses including immunohistochemistry for NUT protein, methylation array, whole genome, and RNA-sequencing was done to confirm the presence of the fusion in the tumor. This is the first description of a pediatric patient with a *ZNF532-NUTM1* fusion, yet the histology of this tumor is similar to that of adult cancers with *ZNF-NUTM1* fusions and other *NUTM1*-fusion positive brain tumors reported in literature. Although rare, the distinct pathology and underlying molecular characteristics of these tumors separate them from other embryonal tumors. Therefore, the *NUTM*-rearrangement appears to define a novel subgroup of pediatric central nervous system embryonal tumors with rhabdoid/epithelioid features that may have a unique response to treatment. Screening for a *NUTM1*-rearrangement should be considered for all patients with unclassified central nervous system tumors with rhabdoid features to ensure accurate diagnosis so this can ultimately inform therapeutic management for these patients.

Keywords

ZNF532-NUTM1, embryonal tumor, pediatric, brain tumor, optical genome mapping, fusion

Introduction

Embryonal tumors are a class of highly aggressive and heterogenous malignant central nervous system (CNS) tumors that primarily occur in infants and young children [1]. They are characterized histologically as undifferentiated or poorly differentiated tumors of neuroepithelial origin and have high cellular activity and rapid growth. There are several types of embryonal tumors including medulloblastoma and other embryonal tumors including atypical teratoid rhabdoid tumor (AT/RT) and embryonal tumors with multilayered rosettes (ETMR)[2,3]. To assist in distinguishing between the different classifications of embryonal tumors, genetic characterization, which has rapidly become part of the diagnosis workflow, is essential. Medulloblastoma is further subdivided into four categories: WNT-activated, SHH-activated, Group 3 (non-WNT/non-SHH), and Group 4 (non-WNT/non-SHH)[4]. ETMR tumors, which are rare and generally arise in infants, are mostly classified through the presence of multilayered neuroepithelial cells that resemble rosettes with or without the presence of C19MC alteration[5]. For AT/RTs, SMARCB1 (also called INI1) or less commonly SMARCA4 (BRG1) loss of function is a criterion for diagnosis[6]. CNS neuroblastoma, FOXR2- activated and CNS tumor with BCOR internal tandem duplication are embryonal tumors that have recently been added to the 2021 WHO classification guidelines based on their molecular signatures[3]. Tumors that have histologic features of AT/RT, but do not have either INI1 or BRG1 loss were classified as CNS embryonal tumors with rhabdoid features based on the 2016 WHO guidelines, and now are included in the CNS embryonal tumors, NOS category [1–3]. The tumors in this last subgroup do not have known/common molecular features.

Standard of care therapy for patients with embryonal tumors generally includes a combination of surgery, chemotherapy and radiation therapy[7–9]. Historically, therapeutic management primarily depended on patient characteristics such as age, tumor location, presence of metastatic disease and tumor histology (i.e. medulloblastoma vs AT/RT, etc). More recently, molecular characteristics of the tumors have introduced novel treatment options for patients with specific tumor alterations. For example, hedgehog pathway inhibitors are being included in clinical trials for patients with SHH-activated medulloblastoma, lower radiation doses are being trialed in patients with lower-risk WNT-activated medulloblastoma, and intensified therapies are being trialed in patients with high-risk embryonal tumors[9]. An accurate histological and molecular diagnosis of embryonal tumors is therefore very important for both risk stratification and treatment planning.

In this case, the patient presented with an unusual tumor that had histopathologic features best aligning to a CNS embryonal tumor with rhabdoid features. Optical genome mapping (OGM) revealed a novel *ZNF532-NUTM1* fusion that has not been described previously in children with any cancer type or adult brain tumor but has been identified in adults with tumors of the lung, mandible, parotid gland, and pelvic bone that have similar histologic features as the patient's tumor. This case report describes clinical and genomic features of a patient with this novel pediatric embryonal tumor subtype.

Case presentation

The patient was a male between 0-5 years of age and presented to care with stalled development, drooling, left-sided face flushing, left-sided eyelid drooping and daily complex partial seizures. MRI imaging revealed a cystic mass with an enhancing nodular component measuring 11x13 cm in the temporoparietal region (Figure 1A&B). Diffusion weighted imaging was consistent with a cellular lesion. MRI of the spine was negative for metastatic disease. A gross total resection (GTR) was performed without complication three days later (Figure 1C). On pathology, the tumor was a high-grade neoplasm with focal necrosis (Figure 1D). Undifferentiated cells with an embryonal morphology were the primary cell type, but there were also slightly larger cells with epithelioid or rhabdoid morphology (Figure 1 E&F). Mitotic figures were noted to be abundant (Figure 1E) and the tumor had a high proliferative index (Figure 1G). Immunohistochemistry (IHC) showed patchy GFAP, EMA and cytokeratin staining. p53 IHC staining was consistent with wild type and INI1 was retained (Figure 1H). Further IHC analysis showed retained BRG1, which ruled out an AT/RT. The patient was diagnosed with a WHO Grade IV CNS embryonal tumor with rhabdoid features based on the 2016 classification criteria[2].

The patient was treated with standard infant embryonal tumor chemotherapy (Cisplatin, Vincristine, Etoposide, Vincristine, Cyclophosphamide, Methotrexate) followed by 3 cycles of high-dose consolidation chemotherapy with stem cell rescue (Carboplatin, Thiotepa and Etoposide). The patient had good response to the induction

chemotherapy with no evidence of disease noted on the pre-consolidation MRI. During consolidation cycle #1, the patient developed hypotension and veno-occlusive disease of the liver. Despite maximum intervention, the patient passed away approximately one week later.

Because of the patient's early presentation with a unique tumor, the cancer genetics team was consulted to rule out possible germline cancer predisposition. Family history was significant for a sibling who died in utero, and distant history of leukemia, cervical cancer, colon and breast cancer on the maternal side of the family. A germline tumor panel including approximately 120 genes was performed and revealed a variant of unclear significance in the *MC1R* gene and a maternally inherited *PTCH1* gene mutation that was initially a variant of unclear significance but has subsequently been reclassified as a likely benign variant. Neither of these germline gene mutations were thought to be associated with his tumor development.

Molecular characterization

Tumor analysis was performed on a research basis and included Epic methylation array, Optical Genome Mapping, whole genome sequencing, and RNA sequencing (See supplementary file for methods). The EPIC methylation array results were entered into the tumor methylation classifier (MolecularNeuropathology.org) but the tumor did not cluster with any of the commonly diagnosed embryonal tumors (not classifiable) [10]. Whole genome sequencing analysis for single nucleotides and small insertions/deletions did not reveal significant Tier1 or Tier 2 somatic mutations. The tumor mutation burden was calculated to be <1 mut/Mb (low) and a majority of the variants identified were noted to be intronic.

Optical genome mapping (OGM; Bionano Saphyr Instrument), which utilizes ultra-long DNA molecules to assess for structural variants, showed complex three-way rearrangements amongst chromosomes 12, 18 and 15 in the tumor (Supplementary Figure 1). The most clinically significant event was an insertion that resulted in the fusion of *ZNF532* on chromosome 18 with *NUTM1* on chromosome 15 (Figure 2A). Additional rearrangements without clear clinical significance included (1) a translocation between chromosome 15 and 18; (2) an inversion on chromosome 18 near the same breakpoint as the translocation; (3) copy number variant change on chromosome 15 and (4) a small insertion on chromosome 18 derived from chromosome 12 (Supplementary Figure 2). Subsequent SV analysis of the whole genome sequencing data and additional RNA-sequencing confirmed the presence of the *ZNF532-NUTM1* fusion in the tumor (Figure 2B&C). No other clinically significant SVs or fusions were identified.

In order to better understand the role and frequency of *ZNF532-NUTM1* fusions in pediatric brain tumors, a literature review using Pubmed was performed with a series of search strings including *ZNF532-NUTM1*, *NUTM1* AND brain tumor, and *ZNF532* AND brain tumor. The search was limited to English language articles concerning human studies exclusively and with publication dates going back 15 years from March 2022. Five additional cases with a *ZNF-NUTM1* fusion (four with *ZNF532*, one with *ZNF592)* and five reports of patients with *NUTM1*-rearranged brain tumors were identified (Figure 3A and Table1). *NUTM1* fusions in brain tumors are rare but have been identified in children and adults with supratentorial small-cell tumors similar to our patient (Table 1) [11–14]. The specific *ZNF532-NUTM1* fusion identified in our patient has not been reported in a child or a patient with a brain tumor prior to this case. However, this has been associated with adult lung, mandible, parotid gland, and pelvic bone cancers that have round cell and/or undifferentiated epithelioid morphology with or without a rhabdoid cell component, comparable to our patient's tumor (Figure 3A, Figure 1D-F) [15–19].

The patients reported in literature had a variety of different treatments. A multimodality treatment approach using surgery along with radiation, chemotherapy or both was most commonly employed, similar to the approach used with our patient. The one year overall survival was 40% and 45% in the *NUTM1*-rearranged brain tumor group and *ZNF532-NUTM1* cancer group respectively (Figure 3B).

An analysis of embryonal (n= 19) and AT/RT (n= 29) samples available through the Children's Brain Tumor Network database did not reveal any additional tumors with a *ZNF532-NUTM1* fusion or a *NUTM1*- or *ZNF532*-rearrangement. However, this is a limited dataset and none of these tumors had pathology similar to the patient in this report. Additional analysis of a larger cohort of samples with round cell tumors and rhabdoid/epithelial features would be helpful to determine the frequency of these fusions in pediatric brain

tumors.

Discussion and Conclusions

Molecular characterization of pediatric brain tumors can help with both diagnostic and prognostic stratification. This has helped improve therapeutic strategies for patients with many tumors including embryonal tumors such as medulloblastoma and AT/RT. In this patient's case, the tumor was described as an embryonal tumor with rhabdoid/epithelioid features that did not have genomic characteristics of an AT/RT and therefore was diagnosed under the umbrella term CNS embryonal tumor with rhabdoid features. Through optical genome mapping and subsequent whole genome and RNA sequencing, we uncovered a *ZNF532-NUTM1* mutation, which, based on previous reports in literature and the patient's genomic and histologic findings, was most likely the genomic driver in this patient's tumor.

NUTM1, is the *NUT* midline carcinoma gene family member 1 and located on chromosome 15q14[20]. *NUTM1*- rearranged tumors have a chromosomal translocation resulting in the fusion of the *NUTM1* gene on chromosome 15 with a gene involved in transcription regulation. The most common fusion partner is *BRD4* (chromosome 19) but fusions involving *BRD3* (chromosome 9), *NSD3* (chromosome 8) and zinc finger genes (*ZNF*) such as the *ZNF532* (chromosome 18) seen in our patient have also been described[20]. *NUTM1* rearrangements are most commonly associated with sarcomas and hematologic malignancies in both children and adults, although a variety of other cancers have also been identified. Children and infants with *NUTM1* fusions in B-cell ALL have favorable prognosis, while the clinical impact of this fusion on sarcomas is still unclear[20,21].

Although the oncogenic impact of the *ZNF532-NUTM1* fusion in CNS tumors has not been studied, functional studies of other cancers have shown that *NUTMI*-fusion positive cells demonstrate lack of differentiation of epithelial cells and nuclear localization of the NUT protein, suggesting that *NUTM1*-fusions contributed to tumor development by associating with nuclear chromatin and interfering with cell differentiation [22,23]. Consistent with this finding, nearly all of our patient's tumor cells displayed homogenous nuclear expression of the monoclonal NUT antibody confirming nuclear localization of the NUT protein in this tumor (NeoGenomics; Figure 1I). *NUTM1*-rearranged tumors have also been described as having a lower mutation burden than other cancers, with an abundance of intronic mutations that do not affect canonical oncogenes or tumor suppressor genes[24,25]. This is consistent with the patient's whole genome sequencing results that primarily showed intronic mutations with a low mutation burden and no other Tier1 or Tier2 pathogenic mutations.

Standard therapy for pediatric embryonal tumors includes a combination of surgery, radiation therapy and chemotherapy. The patient presented in this report had GTR followed by three cycles of induction chemotherapy and then one cycle of high dose chemotherapy followed by stem cell rescue before passing away from treatment complications. The patient had no radiographic evidence of disease at the time of passing. Upon review of CNS cases with *NUTM1*-fusions (Table 1) and patients with *ZNF532-NUTM1* associated cancers (Figure 3A), most patients had similar multi-modality treatment including surgery, RT and chemotherapy. Surgery, with the goal for GTR and negative margins, was performed when possible and has been shown to have a positive impact on overall outcomes in some patients with midline (head and neck) *NUT*-rearranged tumors [26–28]. Radiation therapy has also been shown to have some benefit in patients with *NUTM1*-rearranged midline tumors and has primarily been used in older patients with localized disease[26]. Chemotherapy has had mixed responses and thus far has not been demonstrated to improve overall outcomes in patients with these tumors[20,27]. However, a standardized therapeutic approach has not yet been identified in children or adults with *NUT*-rearranged tumors, so additional studies would be required to fully understand the role of surgery, radiation therapy, and chemotherapy in patients with these tumors.

In this report, we describe a novel pediatric brain tumor subtype with *NUTM1*-fusion positive pediatric CNS tumors, including the *ZNF532-NUTM1* fusion associated with rhabdoid/epithelial features on pathology. Although these tumors are rare, their distinct pathology and underlying molecular characteristics will likely separate them from other embryonal tumors in terms of response to treatment and targeted therapeutic options. Screening of CNS embryonal tumors that cannot be classified as medulloblastoma, AT/RT, ETMR or another molecular subgroup for the NUT protein through IHC followed by SV analysis either though WGS, RNA-

sequencing or OGM to identify the specific *NUT*-rearrangement would be helpful for the identification of tumors that fit within this subgroup. Additional studies are needed to develop the best therapeutic options for these patients.

Methods

Sample processing

Ultra-high molecular weight (UHMW) DNA was extracted following manufacturer's guidelines (Bionano Genomics Inc, USA) from flash frozen brain regions (superior frontal gyrus and primary visual cortex) as well as pelleted frozen PBMCs. Briefly, a total of 15-20mg of brain tissue or 1.5-2 million PBMCs were homogenized in cell buffer and digested with Proteinase K. DNA was precipitated with isopropanol and bound with nanobind magnetic disk. Bound UHMW DNA was resuspended in the elution buffer and quantified with Qubit dsDNA assay kits (ThermoFisher Scientific). Total RNA was extracted using Qiagen RNeasy Kit following manufacturer's guidelines (Qiagen, Germany). RNA sequencing was performed at Novogene Inc, mRNA was selected from total RNA using poly-T oligo-attached magnetic beads and sequenced on an Illumina short-read instrument with 85 million reads (Novogene, USA).
DNA labeling was performed following manufacturer's protocols (Bionano Genomics, USA). Direct Labeling Enzyme 1 (DLE-1) reactions were carried out using 750 ng of purified UHMW DNA. Labeled DNA was loaded on Saphyr chips for imaging. The fluorescently labeled DNA molecules were imaged sequentially across nanochannel arrays (Saphyr chip) on a Saphyr instrument (Bionano Genomics Inc, USA). Effective genome coverage of greater than 500X was achieved for all samples. All samples also met the following QC metrics: labelling density of ~15/100 kbp; filtered (>15kbp) N50 > 230 kbp; map rate > 70%.

Optical genome mapping analysis

Genome analysis was performed using software solutions provided by Bionano Genomics Inc. Automated, OGM specific, pipelines – Bionano Access and Solve (versions 1.7 and 3.7, respectively), were used for data processing and variant calling. **De novo assembly** was performed using Bionano's custom assembler software program based on the Overlap-Layout-Consensus paradigm. Pairwise comparison of all DNA molecules was done to generate the initial consensus genome maps (*.cmap). Genome maps were further refined and extended with best matching molecules. SVs were identified based on the alignment profiles between the *de novo* assembled genome maps and the Human Genome Reference Consortium GRCh38 assembly. If the assembled map did not align contiguously to the reference, but instead were punctuated by internal alignment gaps (outlier) or end alignment gaps (endoutlier), then a putative SV was identified. **Rare variant analyses** were performed to performed to capture mosaic SVs occurring at low allelic fractions. Molecules of a given sample dataset were first aligned against GRCh38 assembly. SVs were identified based on discrepant alignment between sample molecules and reference genome, with no assumption about ploidy. Consensus genome maps (*.cmaps) were then assembled from clustered sets of molecules that identify the same variant. Finally, the cmaps were realigned to GRCh38, with SV data confirmed by consensus forming final SV calls. **Fractional copy number** analyses were performed from alignment of molecules and labels against GRCh38 (alignmolvrefsv). A sample's raw label coverage was normalized against relative coverage from normal human controls, segmented, and baseline CN state estimated from calculating mode of coverage of all labels. If chromosome Y molecules were present, baseline coverage in sex chromosomes was halved. With a baseline estimated, CN states of segmented genomic intervals were assessed for significant increase/decrease from the baseline. Corresponding copy number gains and losses were exported. Certain SV and CN calls were masked, if occurring in GRC38 regions found to be in high variance (gaps, segmental duplications, etc.)

Variant analysis

Bionano Access (Bionano Genomics Inc, USA) was used for SV annotation and filtering. Variants were filtered in access and nanotatoR [29] based on the following criteria: for *de novo*, rare variant and CNV pipelines, SVs were filtered based on Bionano Genomics recommended size and confidence cutoff values (e.g., >500bp/5kbp size cutoff for *de novo* assembly and rare variant pipelines respectively for INDELs). Rare SVs were selected by filtering out common variants with population frequency of >1% using Bionano Genomics' database of SVs

containing >300 healthy individuals. To select for potential clinically significant aberrations a gene list overlapping SVs was used.

Genome sequence analysis

FASTQ reads were aligned to GRCh38 reference genome using, BWA-MEM [30], followed by processing of the aligned bam (for variant calling) using SAMtools [31] and Picard (Broad Institute). Next, for small nucleotide variant (SNV) and small insertion and deletion (INDEL) calling we use Mutect2 [32], followed by annotation using ANNOVAR [33]. Due to absence of a non-tumor tissues from the same individual, we used a 1000 genome panel of normal (PON) variant call file from Broad Institute, as a proxy. Quality filtration for SNV/INDEL was performed using the Mutect2 function. *FilterMutectCalls*. For larger structural variant calls, we used Manta [34], followed by annotation using AnnotSV [35]. For the SV visualization Integrative Genome Viewer (IGV) was used.

RNA-sequence analysis

RNA-seq data was aligned to GRCh38 reference genome, followed by fusion calling using STAR-Fusion [36]. Visualization of the fusion was performed using Clinker [37] and IGV.

EPIC methylation chip analysis

An input of 300 ng of DNA was bisulfite-converted using the DNA Methylation-Lightning kit (Zymo Research). After whole-genome amplification and enzymatic fragmentation, samples were hybridized to BeadChip arrays using the Infinium Methylation EPIC BeadChip kit according to the manufacturer's protocol (Illumina). Intensity values at the over 850,000 methylation sites on the BeadChips were measured across the genome at single-nucleotide resolution using iScan (Illumina). For classifying the tumors, CNS tumor classification tool hosted at molecularneuropathology.org, was used on the methylation signal files [10].

Declarations

Ethics approval and consent to participate

Written informed consent was obtained from the parents of the patient through IRB approved Children's National Hospital protocol, Pro#1339, PI Javad Nazarian, PhD.

Consent for publication

The participant's family provided consent for submission of the case for publication.

Availability of data and materials

Results of all data generated or analysed in this study are either available in the published manuscript or available upon reasonable request. The datasets (including raw data files) used for data analysis during the current study are available from the corresponding author on reasonable request.

Competing interests

H.B. is a part-time employee and a shareholder at Bionano Genomics Inc. E.V. is a shareholder of Bionano Genomics Inc. The remaining authors declare no other competing interests.

Funding

This publication was supported by Award Number UL1TR001876 from the NIH National Center for Advancing Translational Sciences. Its contents are solely the responsibility of the authors and do not necessarily represent the official views of the National Center for Advancing Translational Sciences or the National Institutes of Health.

Authors' contributions

HB, MB and SB analyzed and interpreted the patient genomic data. MB and HB prepared figures and wrote the manuscript. AE was a major contributor to writing the manuscript, the literature search and figure preparation. EP performed literature search and assisted with the figures. MIAS and CR assisted with the pathology interpretation and figures. MK performed the EPIC array methylation analysis. MA assisted with DNA and RNA extraction and analysis. JT, JM, RP and BR participated in patient care. EV and JN provided mentorship with data analysis. All authors read and approved the final manuscript.

Acknowledgements

We would like to acknowledge the patient's family who donated tissue for research.

Figure legends

Figure 1: MRI and IHC images. Axial T2+contrast **(A)** and coronal T1+ contrast (**B)** MRI imaging showed an enhancing supra-insular/inferior parietal mixed cystic/nodular neoplasm. The lesion was completely removed with surgical resection **(C)**. **(D)** H&E staining revealed a high-grade tumor organized in sheets (purple) with areas of necrosis (pale pink) (scale bar = 0.5mm). (E) Mitotic figures were abundant (arrow heads; scale bar = 0.05mm). (F) The undifferentiated tumor cells had an embryonal morphology and scattered larger cells with a vague epithelioid or rhabdoid morphology (arrow in inset shows an epithelioid-like cell; rhabdoid not seen in picture; scale bar = 0.05mm). Ki67 proliferative index was more than 90% (**G**; scale bar 0.05mm). **(H)** INI1 was retained on IHC. **(I)** NUT antibody IHC (NeoGenomics) showed strong nuclear staining of NUT protein (scale bar = 0.1mm).

Figure 2: *ZNF532-NUTM1* fusion identified by optical genome mapping and confirmed by short-read sequencing. (A) OGM genome browser view of the identified fusion. Top: G-band staining of chromosome 18, followed by copy number and structural variant tracks. The green line and adjacent purple dots indicate the location of the insertion and corresponding breakpoints aligning to chromosome 15. The reference chromosomes 18 and 15 are shown in blue, with black vertical lines showing the DLE1 label locations. The assembled sample map is displayed in yellow, the red labels in the middle don't have alignment to chromosome 18, instead they align to chromosome 15. The total insertion size from chromosome 15 to 18 is approximately 200kb. The left breakpoints on both chromosomes is magnified to show annotations of *ZNF532* and *NUTM1* genes, approximate breakpoint location and exons fused to exons. **(B)** Short-read sequencing alignments to the breakpoint location indicated by OGM. Read-pairs maps to two different chromosomes (chr18 and chr15), to confirm the identified translocation between an intron near *ZNF532* and exon 3 on *NUTM1* genes, respectively. **(C)** RNA-sequencing alignments also confirm the exon-exon fusion between *ZNF532* (exon 10) and *NUTM1* (exon3). The split reads are designated by color, with part of the reads mapping to exon 10 of chromosome 18 and other part mapping to exon 3, chromosome 15. The red dotted lines differentiate the 2 chromosomes.

Figure 3: NUTM1 fusion tumors. (A) Oncoplot showing cancers with *ZNF-NUTM1* fusions. Ages are given as a 5 year range. **(B)** Kaplan-Meier curve showing overall survival of brain tumors with *NUTM1*-rearrangements (red line) and *ZNF-NUTM1* cancers (blue line).

Supplementary Figure 1: Representation of the SVs identified in the case in tumor tissue sample and control blood sample. Four level circos plots displaying chromosomal G-band on the outer level, SVs in the middle (insertions – green, deletions – orange, inversions – cyan, duplications – purple, translocation – purple), followed by CNV track (gains – blue, loss – orange) and inner most circle displaying the translocation connections between the chromosomes.

Supplementary Figure 2: Complex rearrangements observed in the tumor sample. Left: Circos plot summarizing the rearrangements seen between chromosomes 12, 15 and 18 (purple connecting lines). Overall, the reference chromosomes are displayed in blue and the assembled sample maps in yellow. DLE1 label sites are in black. Top: Chromosome 18 genome view around the breakpoints between chromosome 12 and 15. An insertion from chromosome 15 and 12 is observed. Additionally, the chromosome 15 and 18 translocation junction results in an inversion as observed on chromosome 18. Middle: Alignments of labels from chromosome 12 to assembled maps on chromosomes 15 and 18, indicating that this DNA material has been inserted onto chromosome 18. Bottom: Translocations between chromosome 15 and 18 observed by two maps as well as a large CN loss on chromosome 15.

Table 1: Previous cases from brain tumors with NUTM1 fusions

Reference	Age/ Sex	Site	Histology	IHC+	Tx/ Outcome	Fusion
Dickson et al [11]	0-5 yo male	Left parietal	Small round cells. Epithelioid-polygonal cells with a reticular-alveolar pattern and prominent myxoid stroma. Nuclear molding, speckled chromatin and conspicuous mitotic activity.	GFAP (2+, focal), synaptophysin (1+), NUT (5+).	Surgery, Chemo, DOD (12 mo)	*BRD4-NUTM1*
Sturm et al [14]	0-5 yo female	Temporal/ Parietal	Small-cell phenotype, alveolar and fascicular growth	NUT (strong)	Unknown AWD (273 mo)	*CIC-NUTM1*
Sturm et al [14]	0-5 yo female	Frontal/ Parietal	Small-cell phenotype, alveolar and fascicular growth	NUT (strong)	Unknown	*CIC-NUTM1*
Siegfried et al [13]	20-25 yo female	Frontal	Fascicular architecture and chondro-myxoid areas; some neuron-like tumor cells; large nucleoli	NUT, GFAP (strong), p53, CD56.	Surgery, NED (16 mo)	*ATXN1-NUTM1*
Ko et al [12]	25-30 yo female	Right Frontal/ Temporal	Variegated tumor consisting mostly of small epithelioid cells with myxoid or fibrillar background	NUT, CD99, CD56, p53, GFAP (focal), neurofilament (focal).	Surgery, Chemo, DOD (1 mo)	*PARD3B-NUTM1*
This Case	0-5 yo male	Right Temporal/ Parietal	Embryonal cell types, as well as epithelioid or rhabdoid-like cell types	GFAP (focal), Ki-67 high, NUT (strong), p53 wildtype	Surgery, Chemo, DOT (5 mo)	*ZNF532-NUTM1*

GFAP indicates glial fibrillary acid protein; Chemo, chemotherapy; DOD, died of disease; AWD, alive with disease; NED, no evidence of disease; DOT, died of treatment. Ages are given as a 5 year range.

References

1. Pinheiro JAF, de Almeida JCM, Manuel J, Lopes PB. Embryonal Tumors of the Central Nervous System: The WHO 2016 Classification and New Insights [Internet]. 2020. Available from: www.jpho-online.com
2. Louis DN, Perry A, Reifenberger G, von Deimling A, Figarella-Branger D, Cavenee WK, et al. The 2016 World Health Organization Classification of Tumors of the Central Nervous System: a summary. Acta Neuropathologica. Springer Verlag; 2016. p. 803–20.
3. Louis DN, Perry A, Wesseling P, Brat DJ, Cree IA, Figarella-Branger D, et al. The 2021 WHO classification of tumors of the central nervous system: A summary. Neuro-Oncology. Oxford University Press; 2021;23:1231–51.
4. Taylor MD, Northcott PA, Korshunov A, Remke M, Cho YJ, Clifford SC, et al. Molecular subgroups of medulloblastoma: The current consensus. Acta Neuropathologica. 2012;123:465–72.
5. Lambo S, von Hoff K, Korshunov A, Pfister SM, Kool M. ETMR: a tumor entity in its infancy. Acta Neuropathologica. Springer; 2020. p. 249–66.
6. Holdhof D, Johann PD, Spohn M, Bockmayr M, Safaei S, Joshi P, et al. Atypical teratoid/rhabdoid tumors (ATRTs) with SMARCA4 mutation are molecularly distinct from SMARCB1-deficient cases. Acta Neuropathologica. Springer Science and Business Media Deutschland GmbH; 2021;141:291–301.
7. Sin-Chan P, Li BK, Ho B, Fonseca A, Huang A. Molecular Classification and Management of Rare Pediatric Embryonal Brain Tumors. Current Oncology Reports. Current Medicine Group LLC 1; 2018.
8. Gajjar A, Robinson GW, Smith KS, Lin T, Merchant TE, Chintagumpala M, et al. Outcomes by Clinical and Molecular Features in Children With Medulloblastoma Treated With Risk-Adapted Therapy: Results of an International Phase III Trial (SJMB03). J Clin Oncol [Internet]. 2021;39:822–35. Available from: https://doi.
9. Upadhyaya SA, Robinson GW, Onar-Thomas A, Orr BA, Johann P, Wu G, et al. Relevance of molecular groups in children with newly diagnosed atypical teratoid rhabdoid tumor: Results from prospective St. Jude multi-institutional trials. Clinical Cancer Research. American Association for Cancer Research Inc.; 2021;27:2879–89.
10. Capper D, Jones DTW, Sill M, Hovestadt V, Schrimpf D, Sturm D, et al. DNA methylation-based classification of central nervous system tumours. Nature. 2018;555:469–74.
11. Dickson BC, Sung YS, Rosenblum MK, Reuter VE, Harb M, Wunder JS, et al. NUTM1 Gene Fusions Characterize a Subset of Undifferentiated Soft Tissue and Visceral Tumors. American Journal of Surgical Pathology. Lippincott Williams and Wilkins; 2018;42:636–45.
12. Ko K, Kitani T, Harris BT, Anaizi AN, Solomon D, Perry A, et al. A novel PARD3B-NUTM1 fusion in an aggressive primary CNS embryonal tumor in a young adult. Acta Neuropathologica Communications. BioMed Central; 2020.
13. Siegfried A, Masliah-Planchon J, Roux FE, Larrieu-Ciron D, Pierron G, Nicaise Y, et al. Brain tumor with an ATXN1-NUTM1 fusion gene expands the histologic spectrum of NUTM1-rearranged neoplasia. Acta Neuropathologica Communications. BioMed Central Ltd.; 2019.
14. Sturm D, Orr BA, Toprak UH, Hovestadt V, Jones DTW, Capper D, et al. New Brain Tumor Entities Emerge from Molecular Classification of CNS-PNETs. Cell. Cell Press; 2016;164:1060–72.
15. Shiota H, Elya JE, Alekseyenko AA, Chou PM, Gorman SA, Barbash O, et al. "Z4" complex member fusions in nut carcinoma: Implications for a novel oncogenic mechanism. Molecular Cancer Research. American Association for Cancer Research Inc.; 2018;16:1826–33.
16. Agaimy A, Haller F, Renner A, Niedermeyer J, Hartmann A, French CA. Misleading Germ Cell Phenotype in Pulmonary NUT Carcinoma Harboring the ZNF532-NUTM1 Fusion [Internet]. 2021. Available from: www.ajsp.com
17. Chen M, Zhao S, Liang Z, Wang W, Zhou P, Jiang L. NUT carcinoma of the parotid gland: report of two cases, one with a rare ZNF532-NUTM1 fusion. Virchows Archiv [Internet]. Springer Science and Business Media Deutschland GmbH; 2022;480:887–97. Available from: https://link.springer.com/10.1007/s00428-021-03253-9

18. Chien YW, Hsieh TH, Chu PY, Hsieh SM, Liu ML, Lee JC, et al. Primary malignant epithelioid and rhabdoid tumor of bone harboring ZNF532-NUTM1 fusion: the expanding NUT cancer family. Genes Chromosomes and Cancer. Blackwell Publishing Inc.; 2019;58:809–14.
19. Alekseyenko AA, Walsh EM, Zee BM, Pakozdi T, Hsi P, Lemieux ME, et al. Ectopic protein interactions within BRD4-chromatin complexes drive oncogenic megadomain formation in NUT midline carcinoma. Proc Natl Acad Sci U S A. National Academy of Sciences; 2017;114:E4184–92.
20. Luo W, Stevens TM, Stafford P, Miettinen M, Gatalica Z, Vranic S. Nutm1-rearranged neoplasms: A heterogeneous group of primitive tumors with expanding spectrum of histology and molecular alterations: An updated review. Current Oncology. MDPI; 2021. p. 4485–503.
21. Boer JM, Valsecchi MG, Hormann FM, Antić Ž, Zaliova M, Schwab C, et al. Favorable outcome of NUTM1-rearranged infant and pediatric B cell precursor acute lymphoblastic leukemia in a collaborative international study. Leukemia. Springer Nature; 2021;35:2978–82.
22. French CA, Ramirez CL, Kolmakova J, Hickman TT, Cameron MJ, Thyne ME, et al. BRD–NUT oncoproteins: a family of closely related nuclear proteins that block epithelial differentiation and maintain the growth of carcinoma cells. Oncogene. 2008;27:2237–42.
23. Gu B, Hakun MC. Challenges and Opportunities in NUT Carcinoma Research. Genes (Basel) [Internet]. MDPI AG; 2021;12:235. Available from: https://www.mdpi.com/2073-4425/12/2/235
24. Lee JK, Louzada S, An Y, Kim SY, Kim S, Youk J, et al. Complex chromosomal rearrangements by single catastrophic pathogenesis in NUT midline carcinoma. Annals of Oncology. Oxford University Press; 2017;28:890–7.
25. Stirnweiss A, Oommen J, Kotecha RS, Kees UR, Beesley AH. Molecular-genetic profiling and high-throughput *in vitro* drug screening in NUT midline carcinoma—an aggressive and fatal disease. Oncotarget [Internet]. 2017;8:112313–29. Available from: https://www.oncotarget.com/lookup/doi/10.18632/oncotarget.22862
26. Giridhar P, Mallick S, Kashyap L, Rath GK. Patterns of care and impact of prognostic factors in the outcome of NUT midline carcinoma: a systematic review and individual patient data analysis of 119 cases. European Archives of Oto-Rhino-Laryngology. 2018;275:815–21.
27. Chau NG, Hurwitz S, Mitchell CM, Aserlind A, Grunfeld N, Kaplan L, et al. Intensive treatment and survival outcomes in NUT midline carcinoma of the head and neck. Cancer. 2016;122:3632–40.
28. Chau NG, Ma C, Danga K, Al-Sayegh H, Nardi V, Barrette R, et al. An Anatomical Site and Genetic-Based Prognostic Model for Patients With Nuclear Protein in Testis (NUT) Midline Carcinoma: Analysis of 124 Patients. JNCI Cancer Spectrum. 2020;4.
29. Bhattacharya S, Barseghyan H, Délot EC, Vilain E. nanotatoR: a tool for enhanced annotation of genomic structural variants. BMC Genomics. BMC Genomics; 2021;22:1–16.
30. Li H. Aligning sequence reads, clone sequences and assembly contigs with BWA-MEM. 2013;00:1–3. Available from: http://arxiv.org/abs/1303.3997
31. Wysoker A, Fennell T, Marth G, Abecasis G, Ruan J, Li H, et al. The Sequence Alignment/Map format and SAMtools. Bioinformatics. 2009;25:2078–9.
32. Benjamin D, Sato T, Cibulskis K, Getz G, Stewart C, Lichtenstein L. Calling Somatic SNVs and Indels with Mutect2. Available from: https://doi.org/10.1101/861054
33. Wang K, Li M, Hakonarson H. ANNOVAR: Functional annotation of genetic variants from high-throughput sequencing data. Nucleic Acids Research. 2010;38:1–7.
34. Chen X, Schulz-Trieglaff O, Shaw R, Barnes B, Schlesinger F, Källberg M, et al. Manta: rapid detection of structural variants and indels for germline and cancer sequencing applications. Bioinformatics [Internet]. 2016;32:1220–2. Available from: http://www.ncbi.nlm.nih.gov/pubmed/26647377
35. Geoffroy V, Herenger Y, Kress A, Stoetzel C, Piton A, Dollfus H, et al. AnnotSV: an integrated tool for structural variations annotation. Bioinformatics [Internet]. Oxford University Press; 2018;34:3572–4. Available from: http://www.ncbi.nlm.nih.gov/pubmed/29669011
36. Haas B, Dobin A, Stransky N, Li B, Yang X, Tickle T, et al. STAR-Fusion: Fast and Accurate Fusion Transcript Detection from RNA-Seq. bioRxiv [Internet]. 2017;120295. Available from: http://www.biorxiv.org/content/early/2017/03/24/120295?%3Fcollection=

37. Schmidt BM, Davidson NM, Hawkins ADK, Bartolo R, Majewski IJ, Ekert PG, et al. Clinker: visualizing fusion genes detected in RNA-seq data. Gigascience [Internet]. 2018;7. Available from: http://www.ncbi.nlm.nih.gov/pubmed/29982439

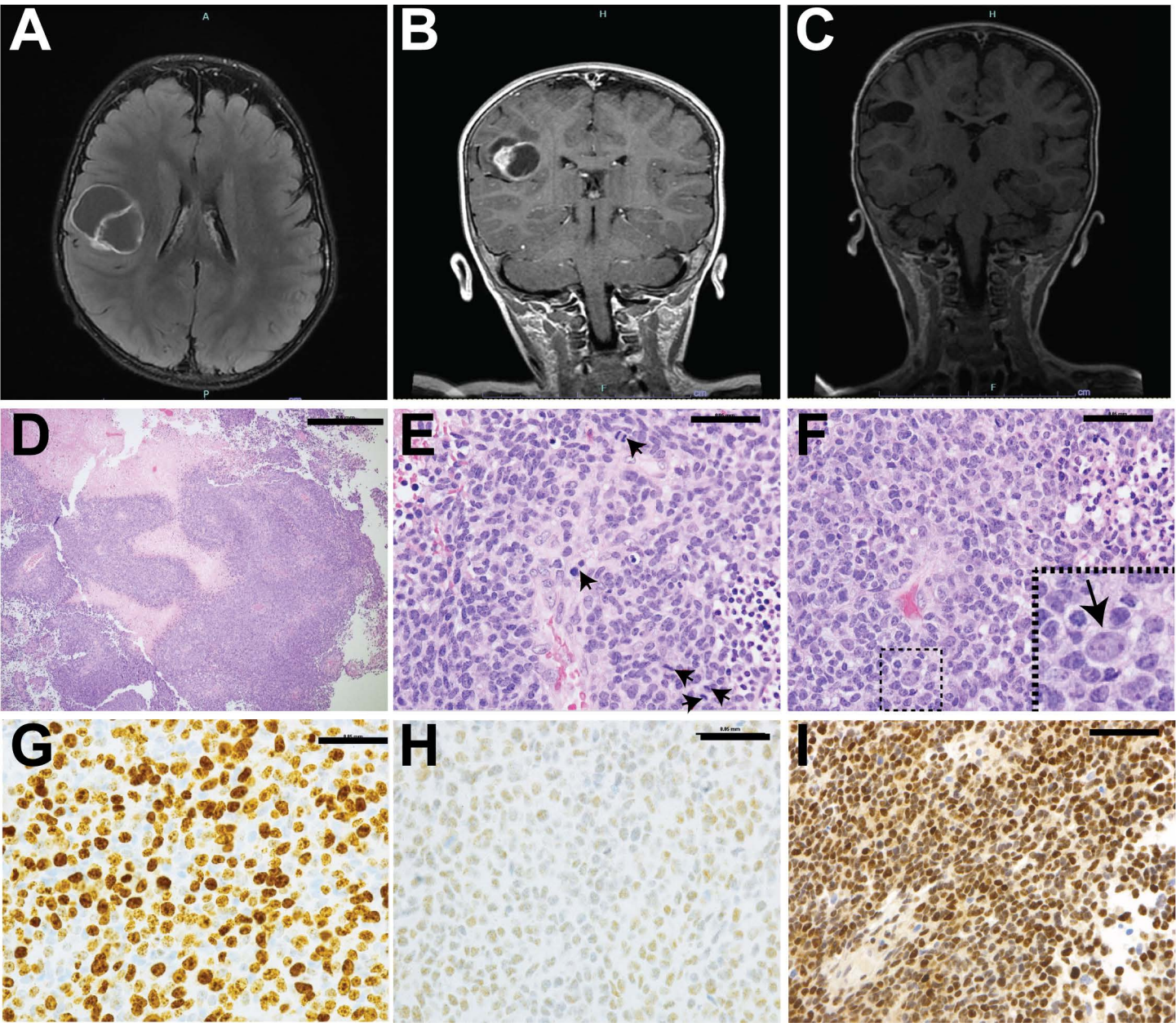
A
B
C
D
E
F
G
H
I

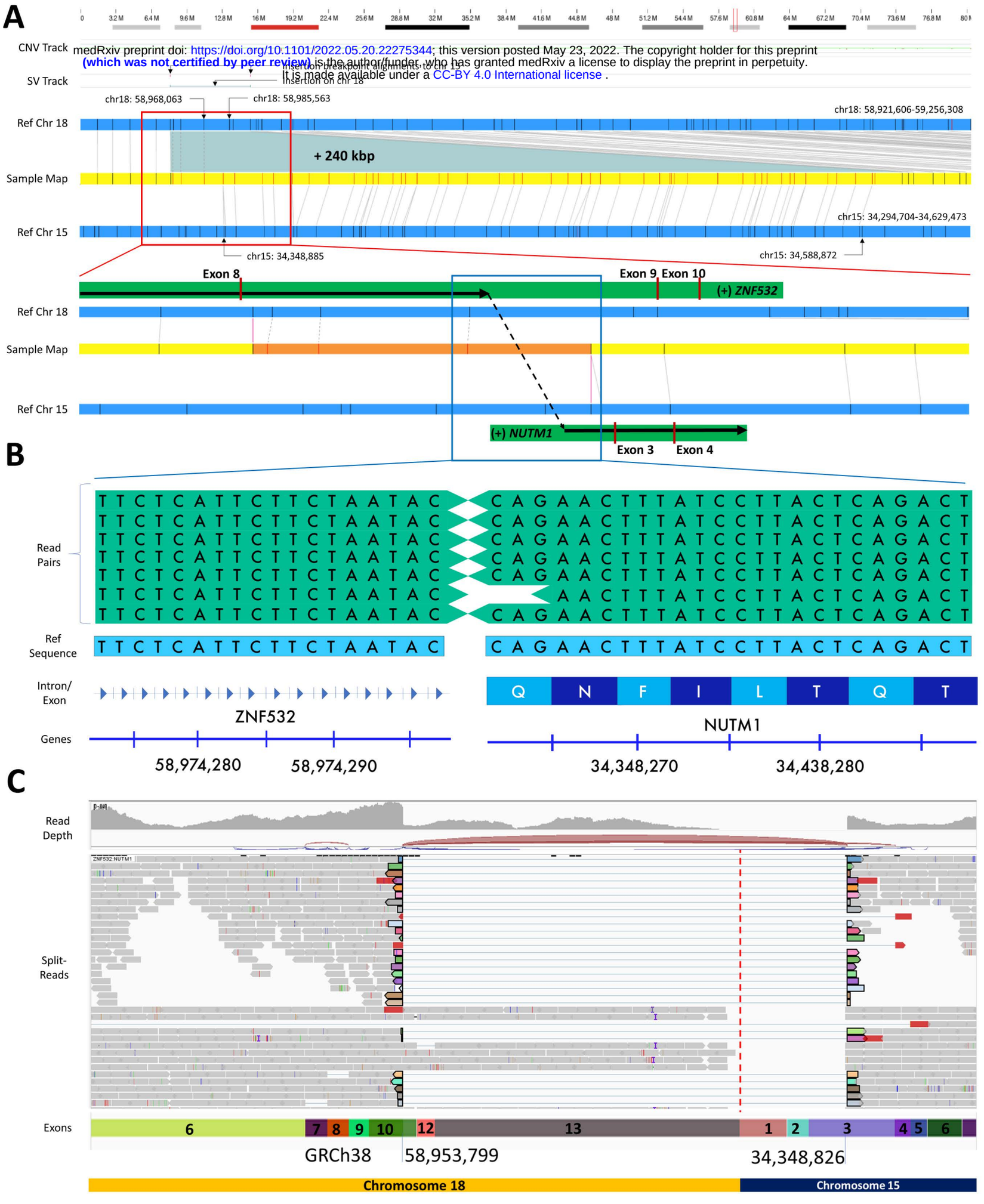

A

Case	Alekseyenko et al. [19]	Shiota et al. [15]	Chien et al. [18]	Agaimy et al. [16]	Chen et al. [17]	This Case
Age/Sex	60-65 F	15-20 F	20-25 F	60-65 F	50-55 F	0-5 M
Survial (months)	1	23	42	34	8	5
Location						
Histology						
Treatment						
Outcome						
Fusion						
Reference	GRCh37/ hg19	hg19	hg19	ND	ND	hg38 Decoy

Histology
- Epithelioid
- Round Cell Malignancy
- Epithelioid/rhabdoid/ focal myxoid
- Round cells/Epithelioid/ rhabdoid/focal myxoid
- Round Cells/squamous
- Round cell/epithelioid/ rhabdoid

Location
- Lung
- Pelvic Bone
- Mandible
- Parotid Gland
- Brain

Treatment
- Biopsy only
- Surgery+Chemo
- Surgery+RT

Outcome
- DOD
- AWD
- DOT

Fusion
- ZNF532 exon4-NUTM1 intron1
- ZNF592-NUTM1
- ZNF532 Exon10-NUTM1 exon2
- ZNF532 exon6-NUTM1 exon5
- ZNF532 exon10-NUTM1 exon3

B

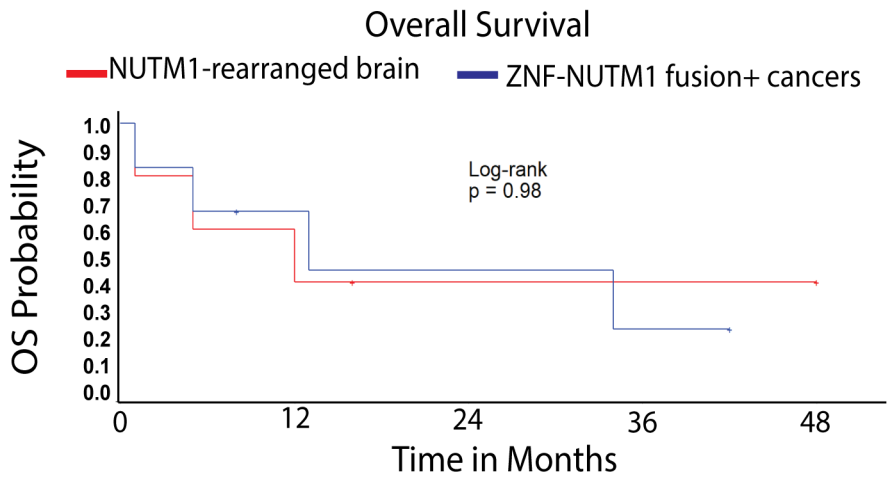

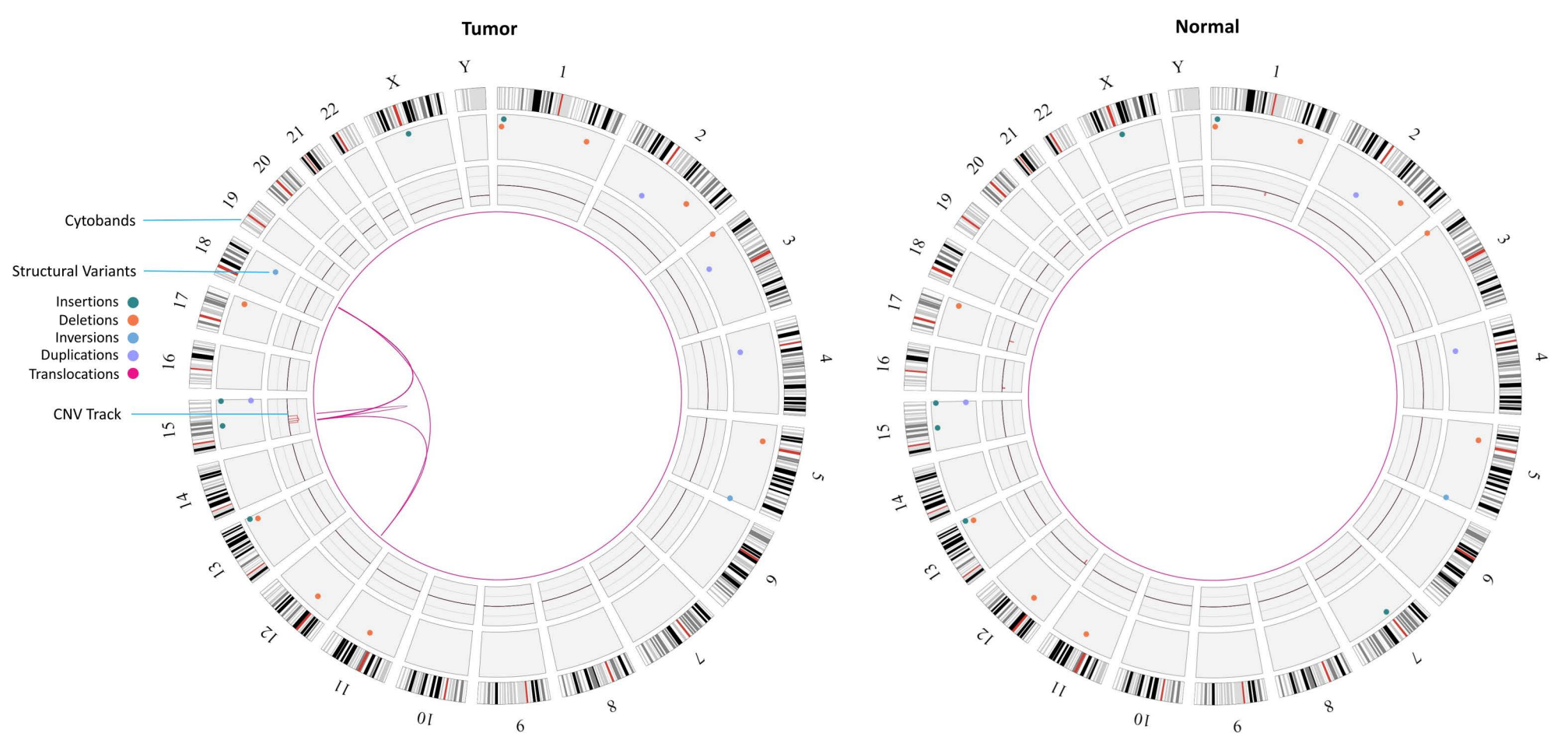
Tumor
Normal
Cytobands
Structural Variants
Insertions
Deletions
Inversions
Duplications
Translocations
CNV Track
X
Y
1
2
3
4
5
6
7
8
9
10
11
12
13
14
15
16
17
18
19
20
21
22

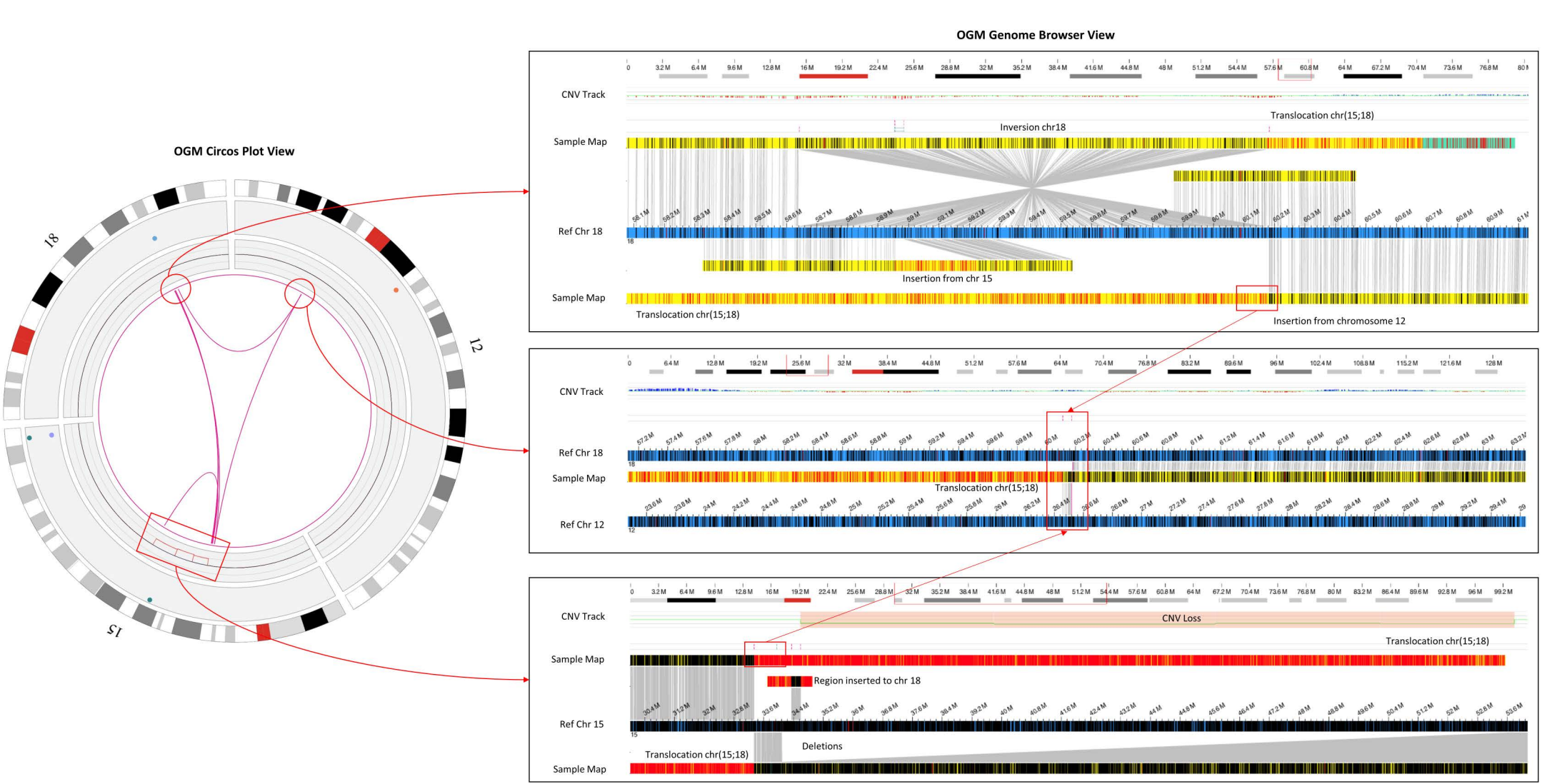
OGM Circos Plot View
18
12
15
OGM Genome Browser View
CNV Track
Translocation chr(15;18)
Inversion chr18
Sample Map
Ref Chr 18
Insertion from chr 15
Sample Map
Translocation chr(15;18)
Insertion from chromosome 12
CNV Track
Ref Chr 18
Sample Map
Translocation chr(15;18)
Ref Chr 12
CNV Track
CNV Loss
Translocation chr(15;18)
Sample Map
Region inserted to chr 18
Ref Chr 15
Deletions
Translocation chr(15;18)
Sample Map